Arboviruses disrupt salivary gland organization and decrease salivation in *Aedes aegypti* mosquitoes

Lucie SOURIAC[1], Mateus BERNI[1], Benjamin VOISIN[2], Carlos F. ESTEVEZ-CASTRO[1,3], Marine LE BERDER[4], Roenick P. OLMO[1], Thiago H.J.F. LEITE[1,3], Hacène MEDKOUR[5], Julien POMPON[5], Eric MAROIS[1], Fabien AUBRY[4] and João T. MARQUES[1]

Affiliations

[1] Inserm U1257, CNRS UPR9022, University of Strasbourg, Strasbourg, France

[2] CNRS UPR3572, University of Strasbourg, Strasbourg, France

[3] Department of Biochemistry and Immunology, Instituto de Ciências Biológicas, Universidade Federal de Minas Gerais, Belo Horizonte/MG, Brazil

[4] CNRS UPR9022, University of Strasbourg, Strasbourg, France

[5] MIVEGEC, Université de Montpellier, IRD, CNRS, 34394 Montpellier, France

Abstract

Aedes aegypti mosquitoes are major vectors for arboviruses. Virus transmission occurs during blood feeding, when infected mosquitoes release both viral particles and saliva. Although saliva proteins can influence viral transmission, their study has been limited by the difficulty of quantifying salivation in natural transmission contexts. Here, we generated a transgenic *Aedes aegypti* line that secretes fluorescent markers into saliva, enabling direct visualization and quantification of salivation. Using this tool, we found that secretion of saliva reporters is robust across diverse physiological conditions but is markedly reduced following Zika or chikungunya virus infection, both in artificial salivation and mouse feeding assays. In the salivary glands, viral antigens displaced saliva reporters in secretory acinar cells, suggesting a segregation mechanism by which the virus is released independently from salivation. Importantly, diminished release of saliva proteins may contribute to the increased probing behavior observed in infected mosquitoes, which can enhance the chances of virus transmission. Together, these findings suggest that virus-induced suppression of salivation may be an adaptive feature that enhances transmission efficiency.

Introduction

Every year worldwide, mosquitoes are responsible for millions of human deaths due to the pathogens they vector. Arboviruses such as yellow fever (YFV), dengue (DENV), Zika (ZIKV) or chikungunya (CHIKV) are transmitted by *Aedes* mosquitoes. Current global warming and urbanization dynamics facilitate the spread of mosquitoes in temperate regions, increasing the risk of arboviruses circulation in these areas[1,2]. If no efficient measures are taken, 60% of the world population is expected to be at risk to contract DENV by the year 2080[2]. The main vector of arboviruses, *Ae. aegypti*, is well adapted to urban landscapes and feeds preferentially on humans[3,4]. It is established in tropical and subtropical regions of the world, allowing the endemic spread of mosquito-borne viruses in these regions[5–8].

Mosquitoes get infected when they blood feed on a viremic vertebrate host. Viruses acquired in the blood infect and replicate in enterocytes in the midgut before disseminating to the hemocoel of the mosquito[9]. Once in the circulation of the mosquito, the virus will infect and replicate in the salivary glands[10]. There, the virus accumulates in specific sites at the apical cavity of acinar cells that appear distinct from vesicles containing saliva[11]. There, the virus is released when the mosquito probes the skin of the next host to blood feed again. Since the virus is released from the salivary glands, it is assumed that transmission is intimately associated with the release of saliva proteins by the mosquito[12]. Saliva has an important role in modulating different aspects of blood feeding on a vertebrate host, being involved in the inhibition of host responses as well as feedback loops that fine-tune mosquito behavior[12]. For example, LIPS proteins in the saliva modify proboscis morphology and proprioception signaling to promote feeding on a vertebrate host[13]. Of note, saliva proteins have been shown to affect arbovirus infections. For example, venom allergen-1 and sialokinin increase the pathogenicity of ZIKV by activating autophagy or vascular leakage at the biting site, respectively[14,15]. In contrast, the D7 saliva protein interacts directly with DENV particles, inhibiting infection[16], and aegyptin activates immune responses in mice, decreasing DENV infection[17]. Natural transmission by the mosquito vector affects the pathogenesis of arbovirus infections compared to artificial injection of the virus[18,19]. These results support a role for mosquito saliva in modulating arbovirus infection in the mammalian host. However, natural infection models with infected mosquitoes have not directly measured the release of saliva[18,19]. Other studies based on co-injection of saliva or salivary gland extracts with the virus assume this is what happens during natural transmission by infected mosquitoes[20,21]. Indeed, tracking the release of saliva proteins and virus by an infected mosquito is a challenge. Some studies have assayed viral transmission using forced salivation, where mosquitoes are immobilized and allowed to salivate in drops of oil[22,23] or tips filled with physiological buffers[24]. These studies provided indirect estimations of the release of saliva proteins analyzing the volume of saliva released or engorgement of the mosquito. In forced salivation assays, a disconnect between the volume of saliva and virus released from mosquitoes has been reported[25]. It also remains unclear whether there is a direct correlation between volume of liquid and the amount of saliva proteins released. These may also help explain why forced salivation assays often underestimate the amount of transmitted virus compared to natural feeding on mice[26,27].

70 Overall, technical limitations have hindered understanding the connection between salivation (e.g.
71 release of saliva proteins) and virus transmission.
72
73 To address these important questions in the field, we developed a transgenic *Ae. aegypti* reporter line
74 expressing epitope-tagged fluorescent proteins in the distal-lateral lobes of the salivary glands. We also
75 introduced signal peptides to these fluorescent proteins that direct their secretion in the saliva. Using
76 this transgenic line, we were able to quantify the release of saliva reporters at the resolution of individual
77 mosquitoes and to characterize basic aspects of the physiology of salivation. Finally, it also allowed us
78 to study the correlation between salivation and transmission of two relevant arboviruses, ZIKV and
79 CHIKV.
80

Results

Generating a transgenic mosquito line to track salivation

To generate a mosquito line that expresses a reporter for salivation, we first searched for genes encoding proteins secreted within the saliva. The *30Ka* (*AAEL010228* encoding SAAG-4) and *30Kb* (*AAEL010235* encoding aegyptin) genes are controlled by a single bidirectional promoter that drives their expression in the distal-lateral lobes of *Ae. aegypti* salivary glands[28,29]. The *30Kb* gene is also expressed in the proximal-lateral lobes to a lesser extent[28]. Using the recent Mosquito Cell Atlas[30], we confirmed that *30Ka* and *30Kb* are specifically expressed in the distal-lateral lobes of the salivary gland of *Ae. aegypti* mosquitoes and the proximal lobes in the case of *30Kb* (**Figure 1a,b**). They were among the top 35 expressed transcripts in the distal-lateral lobes of the salivary glands (**Supplementary table 1**). Significant expression of *30Ka* and *30Kb* was not detected in other mosquito tissues (**Supplementary figure 1a**).The SAAG-4 and aegyptin proteins, encoded by *30Ka* and *30Kb* genes, respectively, are among the top 20 most abundant secreted in the saliva[31,32]. Mass spectrometry analyses show that SAAG-4 and aegyptin are also in the top 10 proteins found in salivary gland extracts[16]. Of note, the *30K* promoter has been used to successfully drive specific transgene expression in the salivary gland of mosquitoes[33,34], but not to track salivation. Here we built a construct with the *30K* promoter maintaining the signal peptides encoded by *30Ka* and *30Kb* genes in fusion with the fluorescent markers mTurquoise2 (mTurq) and enhanced Yellow Fluorescent Protein (YFP), respectively (**Figure 1c**). V5 and HA epitope tags were also inserted to facilitate detection of mTurq and YFP, respectively (**Figure 1c**). DsRed2 was used as a marker for transgenesis driven by a ubiquitous promoter (*AAEL003888*, *polyubiquitin*, *PUb*) on the same *piggyBac* construct (**Figure 1c**), which was randomly inserted into the genome. A mosquito line with a single insertion that was mapped to a non-coding locus on the 3rd chromosome was selected (**Figure 1c** and **Supplementary figure 1b,c**; see methods for details). This line, named Fudgel, was further characterized.

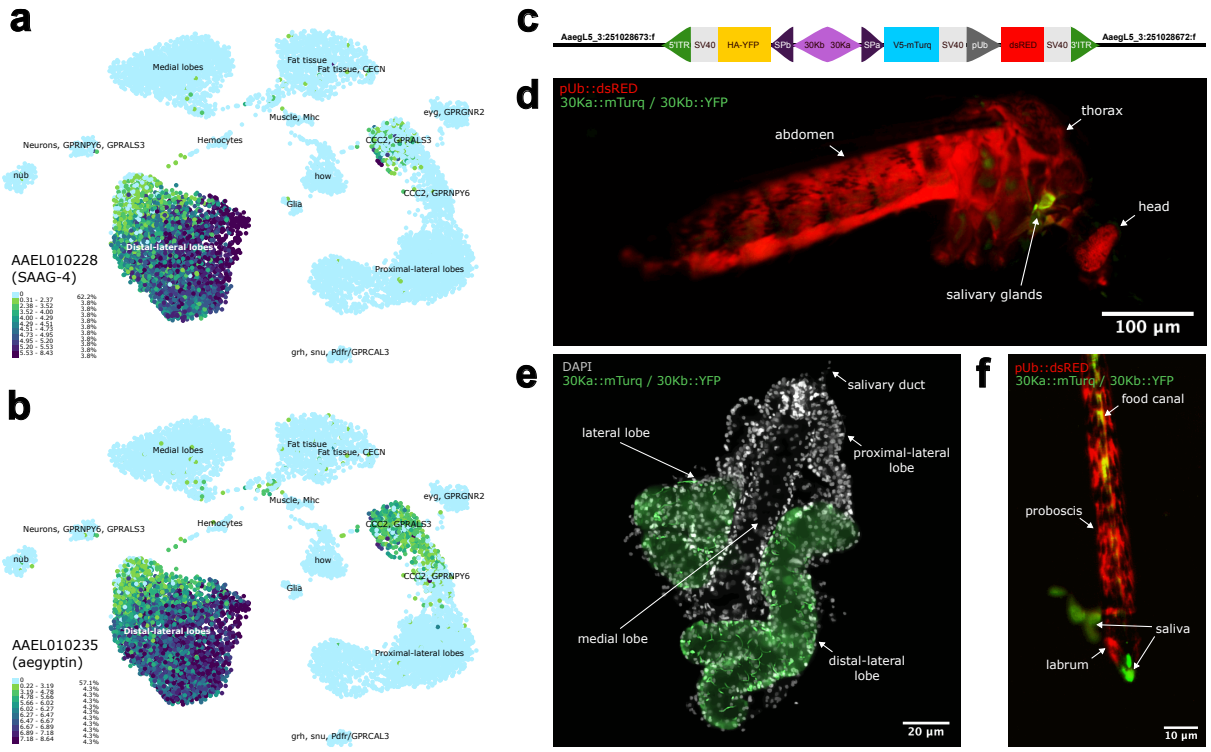

Figure 1- Characterization of the Fudgel transgenic mosquito line to track salivation.

a-b) UMAP representation of *30Ka* (*AAEL010228*/SAAG-4) (**a**) and *30Kb* (*AAEL010235*/aegyptin) (**b**) expression patterns in *Ae. aegypti* snRNAseq data from salivary glands generated with the UCSC Cell Browser[30]. **c**) Fudgel transgenic construct and insertion locus in the *Ae. aegypti* Bangkok genome. The construct is composed of the bidirectional *30K* promoter (*30Ka* and *30Kb*) and their associated endogenous signal peptides (purple and dark purple). *30Ka* drives the expression of the *mTurq* gene tagged in 5' with a V5 tag and followed by a SV40 transcription terminator (blue and grey). *30Kb* drives the expression of the *YFP* gene tagged in 5' with a HA tag and followed by SV40 (yellow and grey). DsRed2 is used as a transgenesis reporter and expressed ubiquitously with a *PUb* promoter and controlled by SV40 (dark grey, red and grey). The construct is flanked by Inverted Terminal Repeats (ITRs) derived from the *piggyBac* transposons and used for transgenesis[35]. The insertion locus of the transgene was identified by Inverse PCR. **d-f**) Expression patterns of the mTurq/YFP (green) and DsRed2 (red) fluorescent markers in whole body (**d**), salivary gland (**e**) and proboscis (**f**) of Fudgel mosquitoes. Nuclei stained with DAPI are shown in **e**.

Characterizing mosquito salivation using the Fudgel reporter line

The analysis of Fudgel mosquitoes on a fluorescent microscope with a green filter - which does not differentiate YFP and mTurq - revealed fluorescent labeled tissue in the mosquito thorax, where the salivary glands are expected to be (**Figure 1d**). In contrast, the DsRed2 fluorescent marker, whose expression is driven by a ubiquitous promoter, labeled the whole mosquitoes (**Figure 1d**). In dissected salivary glands from Fudgel mosquitoes, green labelling was observed in the distal-lateral lobes (**Figure 1e**) as expected using the 30k promoter. Of note, YFP had a broader expression pattern confirming

132 previous observations that *30Kb* is also expressed in proximal-lateral lobes while *30Ka* had a more
133 restricted expression[28]. On a fluorescent microscope, we noted that the mTurq signal was more intense
134 than YFP. This difference may be due to a genomic position effect of the *piggyBac* insertion, since *30Kb*
135 is normally more expressed than *30Ka*[30], and aegyptin is more abundant in saliva than SAAG-4[14].
136 Nevertheless, the expression pattern of the fluorescent proteins in the salivary gland was as expected
137 based on the promoters we used. Since the signal peptides encoded by *30Ka* and *30Kb* are retained
138 in the construct, we next analyzed the presence of the fluorescent markers in the saliva itself.
139 Fluorescent saliva could be observed in green, blue and yellow channels inside the food canal of the
140 proboscis while the walls of the canal are labelled with DsRed2 (**Figure 1f** and **Supplementary Figure**
141 **1d**). A real-time video shows release of the mTurq fluorescent marker during salivation on a Petri dish
142 (**Supplementary video 1**). These results suggest that Fudgel mosquitoes produce and secrete
143 fluorescent markers in in the saliva. Although the markers are specifically produced by the distal-lateral
144 lobes, proteins from all lobes are represented in the saliva (**Supplementary table 2**)[14,30]. Therefore, the
145 release of the fluorescent markers should allow direct tracking of salivation.
146
147 To quantitatively monitor the release of saliva proteins by individual mosquitoes, we measured levels
148 of fluorescent markers by western blot using a forced salivation protocol (**Figure 2a**). V5-mTurq could
149 be readily detected after 30 minutes of forced salivation in about half of the mosquitoes tested (**Figure**
150 **2b,c**). Neither the marker levels nor the proportion of individuals with detectable markers - together
151 referred to as salivation performance - changed significantly at 0.5, 1 and 2 hours of forced salivation
152 (**Figure 2c**). Of note, HA-YFP was not detected by western blot (**Figure 2b**) consistent with the
153 microscopy results that suggested it is not as abundant as V5-mTurq. Using V5-mTurq as a reporter for
154 the amount of saliva proteins, we next analyzed the salivation performance of individual mosquitoes at
155 different stages of completion of their gonotrophic cycle. Blood-fed Fudgel mosquitoes were analyzed
156 at different days post-feeding (dpf) (7 dpf, 10 dpf or 14 dpf) with or without egg laying compared to
157 sugar-fed individuals (**Figure 2d**). Overall, the physiological state of the mosquito did not affect
158 salivation performance (**Figure 2e**). There was a significant decrease in saliva levels at 10 dpf in
159 mosquitoes that were allowed to lay eggs and thus completed their gonotrophic cycle (**Figure 2e**). This
160 tendency at day 10 was observed in three out of four independent replicates indicating a physiological
161 difference rather than experimental variation (**Supplementary figure 4**). This observation is in
162 agreement with previous reported variations in host seeking and blood feeding behavior at different
163 stages of the gonotrophic cycle[36]. We also quantified levels of the fluorescent marker remaining in the
164 salivary glands after salivation (**Figure 2f**). No significant differences in markers levels - mTurq and
165 YFP - were observed in salivary glands, compared to control mosquitoes after blood-feeding on mice
166 or forced salivation (**Figure 2g**). These results suggest that levels of saliva proteins released in both
167 natural and artificial salivation settings are relatively small compared to what remains in the glands.
168

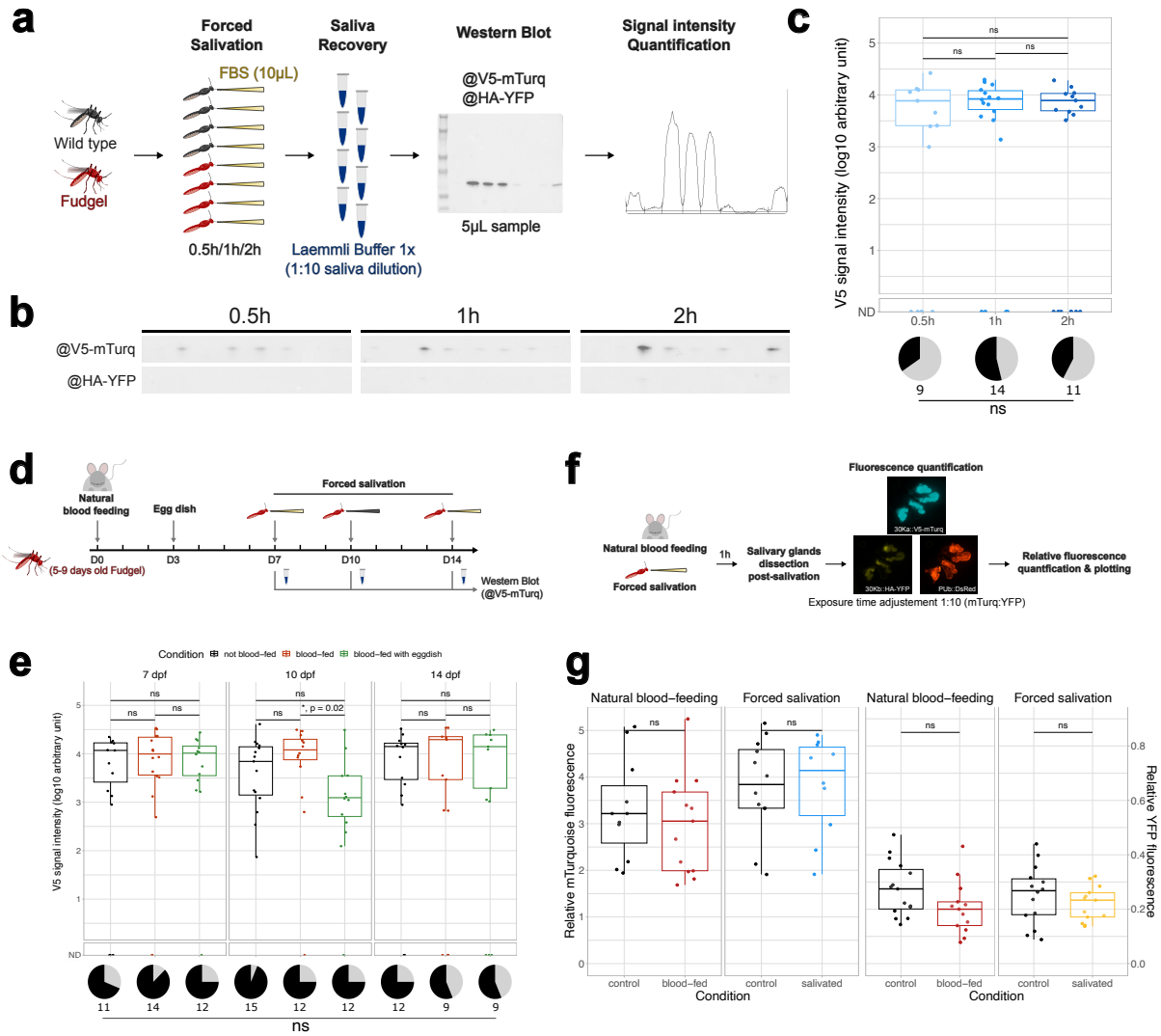

Figure 2- Fluorescence marker detection can be used as a reporter for salivation performance

a) Experimental design for detection and quantification of marker expression after forced salivation. **b**) Western Blot signal for V5 and HA in individual saliva samples of Fudgel mosquitoes after 0.5h, 1h or 2h of forced salivation. **c**) V5 signal intensity in individual saliva samples of Fudgel mosquitoes at different times (n = 20 saliva samples per time point) (log10 scale). Pooled results from independent replicates (N = 3). Individual western Blot results are shown in **Supplementary figure 2** and the raw data in **Supplementary table 3**. **d**) Experimental design for testing the effect of different physiological states on salivation. **e**) V5 signal intensity in individual saliva samples of Fudgel mosquitoes in different physiological states after 1h of forced salivation (n = 16 per condition) (log10 scale). Pooled results from independent experiments (N = 4). Individual western Blot results are shown **Supplementary figure 3,** individual plots in **Supplementary figure 4** and the raw data in **Supplementary table 4**. **f**) Experimental design for testing the effect of salivation on salivary glands. **g**) mTurq and YFP fluorescence intensity relative to DsRed2 (CTCF(marker/DsRed2)) in individual salivary glands of Fudgel mosquitoes 1h after blood-feeding on mice or forced salivation. Exposure time was 10-fold higher for YFP compared to mTurq. Representative images are shown in **Supplementary figure 5** and the raw data in

186 **Supplementary table 5**. Comparison of signal intensity: Kruskal-Wallis test, threshold 0.05.
187 Comparison of prevalence of salivation: Fisher's exact test, threshold 0.05.
188
189 The interaction between mosquito saliva proteins and skin cells after biting has been thoroughly studied
190 *in vitro* using mammalian cell lines or recombinant proteins[37–39]. However, *in vivo* analyses are harder
191 to perform due to the lack of tools to precisely identify and isolate mosquito biting sites and track saliva
192 proteins. Tracking mosquito salivation on a mammalian host after biting would allow precise monitoring
193 of viral replication sites and local immune responses. Since we observed active release of mTurq during
194 forced salivation on a Petri dish (**Supplementary video 1**), we next tested whether the fluorescent
195 markers could be detected directly in human skin explants exposed to mosquitoes (**Figure 3a**).
196 Mosquitoes actively probed the skin explants but could not feed on the human skin biopsies likely due
197 to blood coagulation and/or blood vessel collapse within the 3 hours between surgery and the
198 experiment (**Figure 3b**). Fluorescence microscopy allowed visualizing mosquito bite sites via tracking
199 mTurq and YFP fluorescence markers immediately after probing (**Figure 3c**). Of note, DsRed2
200 expressed under a ubiquitous promoter and lacking a signal peptide was not detected at the bite site
201 (**Figure 3c**). This suggests specific secretion and release of the fluorescent markers expressed under
202 the control of the bidirectional *30K* promoter during probing on the skin explants. Thus, the Fudgel line
203 allows efficient tracking of bite sites and the release of saliva reporters in the skin.
204

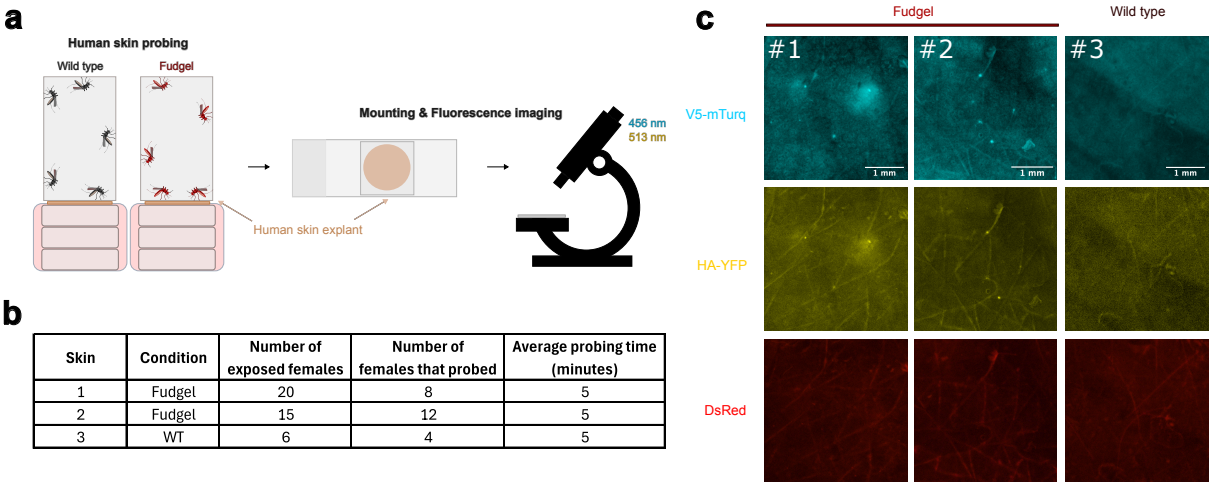

Skin	Condition	Number of exposed females	Number of females that probed	Average probing time (minutes)
1	Fudgel	20	8	5
2	Fudgel	15	12	5
3	WT	6	4	5

205
206 **Figure 3- Fluorescent markers allow tracking of probing sites on human skin**
207 **a**) Experimental design for the analysis of probing on human skin explants. **b**) Mosquito exposure
208 condition and time for each skin explant. **c**) Detection of mTurq and YFP fluorescence at probing foci
209 on each tested human skin explant directly after probing. Exposure time was 10-fold higher for YFP
210 compared to mTurq.
211
212 **Virus transmission and mosquito salivation**
213
214 Mosquito-borne viruses are transmitted by mosquitoes through biting and virus detection in forced
215 salivation assays is often used as a measure of transmission[26,27]. However, in these assays, quantifying

216 the release of saliva proteins is rarely performed due to the lack of experimental tools. Mosquito
217 engorgement with buffer or measurements of the volume of release liquid in oil-filled capillary tubes
218 have both been used as a proxy for salivation[22,23]. To overcome these limitations, we used the Fudgel
219 line to investigate the connection between salivation and virus transmission (**Figure 4a**). In the following
220 assays, mosquitoes were infected with ZIKV by intrathoracic injection to guarantee homogenous
221 systemic dissemination, since we wanted to analyze salivary gland infection and virus presence in the
222 saliva. Viral loads in infected Fudgel mosquito carcasses were not significantly different from non-
223 transgenic controls showing that the transgene does not affect infection (**Figure 4b**). Using a forced
224 salivation protocol, we observed that salivation performance was significantly reduced in ZIKV infected
225 Fudgel mosquitoes, which displayed a lower proportion of individuals with detectable saliva reporter in
226 forced salivation samples (26 out of 40) compared to non-infected mosquitoes (16 out of 16) (**Figure**
227 **4c).** mTurq RNA levels in infected individuals were not significantly different from non-infected controls,
228 suggesting that the effect observed in response to ZIKV infection is due to a decrease in protein levels
229 or release of the saliva reporter (**Figure 4d**). We next measured the presence of infectious virus in the
230 saliva samples from the same individual mosquitoes. Out of 40 tested saliva samples from infected
231 Fudgel mosquitoes, 9 had a cytopathic effect on cells (shown in green on **Figure 4c**). In these samples,
232 we observed no correlation between salivation performance and detection of the virus (**Figure 4c**). Of
233 note, two ZIKV-positive samples had no detectable saliva reporter (**Figure 4c**). To verify if the effect of
234 virus infection on salivation was restricted to ZIKV, we next analyzed mosquitoes infected with CHIKV
235 by intrathoracic injection. Fudgel mosquitoes showed similar CHIKV levels compared to controls,
236 showing no effects of the transgene on viral infection (**Figure 4e**). Similar to ZIKV, we observed a
237 decrease in salivation performance in CHIKV infected mosquitoes with a decreased proportion of
238 salivating individuals (38 out of 54) compared to non-infected controls (19 out of 20), and an additional
239 significant decrease in the amount of detected saliva reporter (**Figure 4f**). Similar to ZIKV, *mTurq* RNA
240 levels in CHIKV infected individuals were not significantly different from non-infected controls (**Figure**
241 **4g**). Out of 54 samples, 5 were infectious on mammalian cells (**Figure 4f**) and again we observed no
242 correlation between virus detection and the amount of detected saliva reporters.
243
244 We next analyzed the effect of virus infection on salivation performance in a mouse model, which is
245 more physiologically relevant. Mosquitoes were given the opportunity to bite naive mice and the release
246 of saliva was directly measured in mouse skin biopsies (**Figure 4h**). Viral loads in infected Fudgel
247 mosquito carcasses were not significantly different from non-transgenic controls after intrathoracic
248 injection of ZIKV (**Figure 4i**). To monitor the release of saliva reporters, we measured protein levels of
249 fluorescent markers in skin biopsies bitten by individual mosquitoes (**Figure 4h**). In this natural
250 salivation model, a decreased proportion of individuals in ZIKV-infected mosquitoes (9 out of 35) had
251 detectable marker release in skin biopsies compared to non-infected controls (14 out of 24) (**Figure 4j**).
252 Of note, engorgement ratios were not significantly different between infected and non-infected
253 mosquitoes, showing that the observed decrease in salivation performance is not due to a modification
254 of the feeding capacity (**Figure 4k**). Together, these results confirm that virus infection decreases the
255 release of saliva reporters by infected salivary glands.

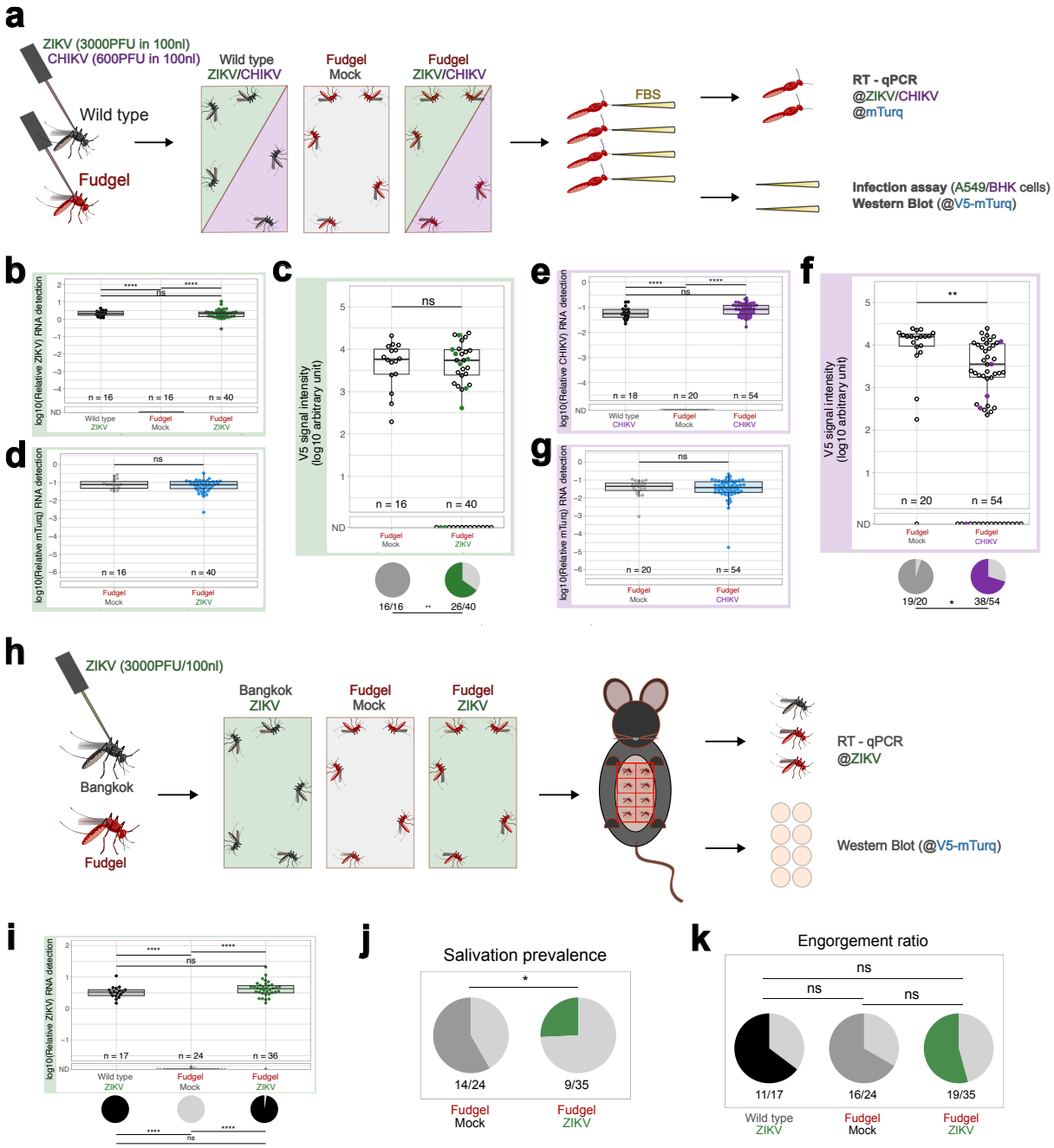

Figure 4- ZIKV and CHIKV decrease salivation in infected mosquitoes

a) Experimental design for the analysis of salivation in mosquitoes infected with ZIKV or CHIKV. **b,e**) Detection of ZIKV (**b**) and CHIKV (**e**) by RT-qPCR in mosquitoes at respectively 14 days and 9 days post infection. **c,f**) V5 signal intensity and salivation prevalence in individual saliva samples of control or ZIKV-infected (**c**) and CHIKV-infected (**f**) mosquitoes. Samples associated with the presence of infectious virus are marked respectively in green and in purple. **d,g**) Detection of V5-mTurq expression by RT-qPCR in control and ZIKV-infected (**d**) or CHIKV-infected (**g**) mosquitoes. **b-f** show pooled results from independent experiments (ZIKV N = 2, CHIKV N = 3). Individual Western Blots are shown in **Supplementary figure 6,** individual plots in **Supplementary figure 7** and the raw data in

268 **Supplementary tables 6** and **7**. **h**) Experimental design for the analysis of mice bitten by mosquitoes
269 infected with ZIKV. **i**) Detection of ZIKV by RT-qPCR in mosquitoes at 15- or 16-days post infection. **j**)
270 Prevalence of individual mouse skin samples displaying V5-mTurq signal by western blot after being
271 bitten by a control or a ZIKV-infected mosquito. Pooled results from independent experiments (N = 2).
272 Individual western Blots are shown in **Supplementary figure 8**. **k**) Engorgement ratio of mosquitoes
273 after 10 minutes of contact with the mouse. Comparison of viral loads in carcasses: Kruskal-Wallis test,
274 threshold 0.05. Comparison of V5 signal intensity and relative mTurq RNA level: Student test, threshold
275 0.05. Comparison of prevalences and engorgement ratios: Fisher's exact test, threshold 0.05.
276
277 **Virus infection disrupts the organization of the saliva reporter in the salivary glands**
278
279 Previous studies have shown changes in the morphology of salivary glands upon infection with
280 CHIKV[11]. To analyze the effect of virus infection on the salivary glands, we analyzed the organization
281 of saliva reporters as well as the segregation of viral antigens by immunofluorescence. Here, we used
282 whole Fudgel mosquitoes embedded in Optimal Cutting Temperature (OCT) compound prior to frozen
283 sectioning on a microtome-cryostat to preserve the organization of salivary glands as much as possible
284 (**Figure 5a**). Whole mosquito sections were analyzed at 15 days post intrathoracic injection of ZIKV to
285 ensure infection of salivary glands. In whole mosquito images, mTurq signal was restricted to salivary
286 glands while ZIKV staining was detected in different parts of the body (**Supplementary figure 9**). In
287 salivary glands, we observed light diffused signal for the saliva reporter that seemed to correspond to
288 the apical cavity of the secretory acinar cells, where saliva proteins are stored (**Figure 5b**). In addition,
289 we observed stronger signal outside of the apical cavity, suggesting accumulation of the reporter in the
290 cytoplasm of acinar cells (**Figure 5b**). This stronger signal of the reporter formed filament-like structures
291 on the lateral and basal sides of the acinar cells that seemed to connect with the salivary duct at the
292 center of the salivary gland (**Figure 5b**). A similar pattern of diffused signal for the saliva reporter in
293 acinar cells was observed in infected salivary glands although the filament-like structures seemed
294 reduced (**Figure 5b**). To quantitate these differences, we used an analysis tool developed for the
295 quantification of mitochondrial filaments using deconvoluted images (**Figure 5c**). This analysis
296 highlighted a significant decrease in the mean area (μm^2) of the saliva reporter filament-like structures
297 in ZIKV-infected compared to non-infected salivary glands (**Figure 5d**). These results show a disruption
298 of the segregation pattern of the saliva reporter in the acinar cells caused by the virus. Furthermore, the
299 loss of mTurq clusters seemed to occur in areas where there was accumulation of the viral envelope
300 protein (Supplementary **Figure 10a**). To investigate this hypothesis, we further analyzed salivary glands
301 displaying the strongest staining for the envelope protein of ZIKV (**Figure 5e** and **Supplementary**
302 **Figure 10b**). Using these images, we calculated Manders' overlap coefficients (M1 and M2) to quantify
303 the colocalization between mTurq and ZIKV. We observed a small fraction of the signal for the ZIKV
304 envelope protein (<0.1) had any overlap with the mTurq filaments, which suggests segregation of the
305 two proteins (**Figure 5f**). A small but more significant fraction of the mTurq filaments (<0.3) overlapped
306 with the signal for the ZIKV envelope (**Figure 5f**). Given that mTurq filaments are uniformly present
307 throughout uninfected salivary glands (**Supplementary Figure 10a),** we may infer that the buildup of

viral antigens during replication in acinar cells leads to the displacement of saliva proteins. That is why the overlap of the ZIKV signal is always low because it only reflects the origin. In contrast, the mTurq signal is everywhere at the start of the infection, which means there is always some overlap with ZIKV antigens.

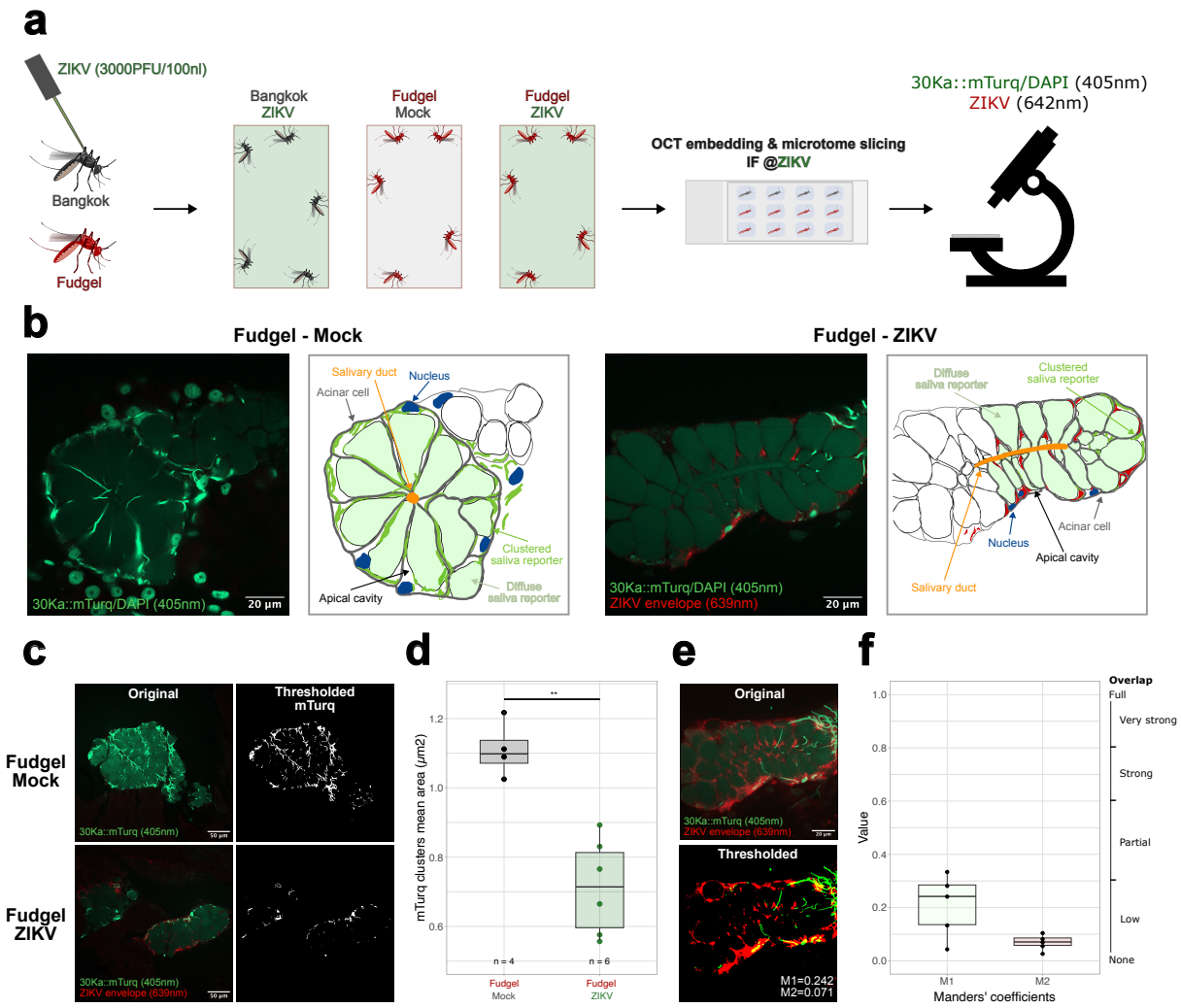

Figure 5- ZIKV infection affects the organization of saliva reporters in infected salivary glands. **a**) Experimental design for immuno-fluorescence analysis of ZIKV-infected mosquitoes. **b**) Representative confocal images of a mock (transverse section) and a ZIKV-infected salivary gland (longitudinal section). A representative scheme highlighting acinar cells (grey), salivary duct (orange), nuclei (blue), saliva reporter (green) and ZIKV envelope (red) is shown on the right. **c**) Representative confocal images of Mock and ZIKV-infected salivary glands showing staining for the saliva reporter (mTurq in green) and the ZIKV E protein (in red). Confocal images ("Original") were deconvoluted using the "Iterative Deconvolve 3D" plugin[40] in ImageJ (20 iterations) and saliva aggregates were highlighted using the "2D Threshold" tool on the "Mitochondria Analyzer" plugin[41] ("Thresholded"). **d**) Mean area (μm^2) comparison between saliva reporter filaments in Mock and ZIKV-infected salivary glands. Wilcoxon test, threshold 0.05. Mock (n = 4) and ZIKV-infected (n = 6). Images of individual salivary glands are shown in **Supplementary figure 10a.** Calculated area values for each individual salivary gland are in **Supplementary table 9**. **e**) Representative confocal image, original and deconvoluted,

327 showing infected salivary glands from Fudgel mosquitoes stained for the salivary gland reporter and
328 the ZIKV envelope protein. **f**) Manders' overlap coefficients indicating the fraction of mTurq that overlaps
329 with ZIKV E staining (M1) and the fraction of ZIKV E that overlaps with mTurq (M2). Individual images
330 and calculations are shown in **Supplementary figure 10b**.
331

Discussion

In this study, we developed a transgenic mosquito line expressing fluorescent markers that function as reporters for saliva proteins. This line allowed us to study basic aspects of the physiology of salivation. We first analyzed the evolution of salivation behavior through a gonotrophic cycle, e. g. from eggs development to their oviposition. We could highlight a transient decrease in salivation performance at 10 dpf for mosquitoes completing of a full cycle, which was observed neither in mosquitoes that were not allowed to lay eggs after feeding nor in those who did not blood feed. Previous studies suggest hormonal variations through the reproduction cycle of female mosquitoes which would be associated with modifications in host seeking and blood feeding behaviors[36]. The observed transient decrease in salivation performance goes along with a decreased host seeking behavior associated with the start of a new gonotrophic cycle. This phenomenon would need to be further characterized, and our tool is a great asset for this purpose. We also measured the effect of natural blood-feeding or forced salivation on salivary glands purging, without detecting any significant difference in saliva content compared to not blood-fed or non-salivating controls. Moreover, this tool allowed us to precisely visualize mosquito probing sites on human skin explants, highlighting its potential use for *in vivo* transmission studies. This could be an important tool to examine skin cells response to saliva components specifically at the biting site, in both non-infected and virus-infected settings. Overall, our results illustrate the potential of the Fudgel reporter line to help gain valuable insights on the physiology of mosquito salivation.

In the context of infection, we showed that both ZIKV or CHIKV decreased mosquito salivation, strongly decreasing the proportion of mosquitoes that secreted detectable levels of saliva reporters. Notably, virus infection disrupted the organization and decreased levels of the saliva reporters in the secretory acinar cells of salivary glands. Of note, viruses did not affect the RNA levels of markers in the salivary gland, thus suggesting a specific effect of these viruses at the protein level. Indeed, others have shown that expression and secretion of saliva proteins can be impacted by virus infection in mosquitoes[42,43]. In addition, our results show that viral antigens are segregated from saliva proteins in infected acinar cells. These observations are in agreement with previous electron microscopy studies of CHIKV-infected salivary glands which suggested that viral particles segregate in separate vesicles from saliva proteins in acinar cells[11]. We propose that as the viral factory is assembled and antigens accumulate, this displaces saliva proteins. Thus, we observe overlap between viral antigens and saliva reporters only at the borders where viral factories are initiating. Then, as the virus replicates and antigens accumulate, saliva proteins are completely gone. As a result of this segregation from saliva proteins, viral particles could presumably be secreted independently. This provides a mechanistic explanation for the disconnection between release of saliva proteins and viral transmission. Importantly, we observed no major damage to acinar cells, this suggesting the cells remain viable, which may be important to allow efficient and continuous virus replication. Our results are in agreement with previous observations that virus titers do not correlate with the volume of saliva released in forced salivation assays[25].

372 Our work represents a shift from the common assumption that viral transmission efficiency correlates
373 with the release of saliva proteins. Of note, genetic depletion of salivary glands or microsurgery removal
374 of the salivary duct caused a reduction in salivation and increased probing behavior in *Anopheles*
375 mosquitoes[44,45]. Thus, reduced release of saliva in virus-infected mosquitoes should lead to an increase
376 in probing and biting behavior. Accordingly, previous studies have shown that dengue-infected
377 mosquitoes have increased biting behavior compared to uninfected controls [46]. This makes sense in
378 light of data showing that successive short probing events resulted in multiple deposition of the virus[46].
379 Damaging the salivary glands could thus be a strategy used by the virus to reduce salivation and
380 increase the probing behavior to enhance viral transmission. A similar situation might occur in
381 *Anopheles* mosquitoes, where there are significant changes in salivary glands morphology and loss of
382 integrity upon *Plasmodium* infection[47]. The authors observed an alteration of saliva composition with a
383 decrease of detected proteins and diffusion of saliva proteins in the mosquito hemolymph. At the same
384 time, no difference was observed in the volume of saliva released from *Plasmodium*-infected
385 mosquitoes although they seemed to probe for longer times[44,47]. Overall, these data suggest that
386 increased probing would serve to increase transmission of pathogens by the mosquito bite. Our results
387 may also help explain recent epidemiological observations that low levels of circulating antibodies
388 against the D7 *Aedes* salivary protein correlate with a higher infection burden of DENV in human
389 populations living in *Aedes* endemic populations[48]. Hence, we propose here a transmission model in
390 which viral infection reduces the secretion of saliva proteins by the mosquito, resulting in increased
391 probing and enhanced delivery of virus particles independently of saliva. Given the disconnect between
392 salivation and release of viral particles, it will be important to further investigate unclear how the virus
393 is delivered during mosquito probing. We believe that the tool we developed here will help answer these
394 questions and help develop strategies to control the transmission of vector borne viruses.
395

396 **Material and methods**
397
398 **Cloning, transgenesis and Fudgel line establishment**
399 Sequences of the 30K bidirectional promoter and associated signal peptides were recovered from the
400 AaegL5 LVP_AGWG reference genome on the VectorBase database
401 (https://vectorbase.org/vectorbase/app) and synthesized as a gBlock gene fragment (IDT). The gBlock
402 sequence was cloned using the NEBuilder® HiFi DNA Assembly Cloning kit (ref E5520S) in a pSKB-
403 plasmid (Addgene #62540), previously linearized by PCR amplification using the ThermoFisher
404 Scientific DreamTaq DNA polymerase (ref EP0701) (primers in **Supplementary table 8**). The
405 sequences for epitope-tagged fluorescent markers were amplified from lab stock plasmids by PCR
406 using the ThermoFisher Scientific Phusion High-Fidelity DNA polymerase (ref F530S) (primers in
407 **Supplementary table 8**). A backbone plasmid containing the PUb::DsRed2::SV40 sequence was
408 digested using BamHI and SmaI restriction enzymes (ThermoFisher). The final construct was
409 assembled using NEBuilder® HiFi DNA Assembly Cloning kit (ref E5520S). Full plasmid sequence is
410 provided in **Supplementary Table 8**.
411
412 This plasmid was injected at a concentration of 300 ng/µL in mosquito eggs with 100 ng/µL of a helper,
413 codon-optimized *piggyBac* transposase-expressing plasmid[35] (available on request) in 0.5x PBS as
414 follows: *Ae. aegypti* female mosquitoes of the Bangkok strain were blood-fed 4 days prior to injection
415 and allowed to lay eggs. One hour-old eggs were aligned along wet nitrocellulose on a microscope slide
416 and injected in their posterior pole using a Nikon ECLIPSE TE2000-S inverted microscope, Eppendorf
417 Femtojet 4x micro-injector and Eppendorf TransferMan NK2 control panel. Injected G0 larvae were
418 screened and individuals displaying transient DsRed2 fluorescence expression were backcrossed to
419 wild-type Bangkok mosquitoes. From their G1 progeny, DsRed2-positive individuals were selected
420 under a fluorescent binocular microscope (Nikon SMZ18 microscope, sola light engine Lumencor® light
421 source), backcrossed, and progeny was again individually backcrossed. In G3, populations showing
422 50% inheritance of the transgene were selected, suggestive of a single transgene insertion. Positive
423 G3 mosquitoes of a given population were self-crossed. Homozygous – single insertion – G4
424 mosquitoes were sorted based on fluorescence intensity using the COPAS instrument[49] to generate the
425 Fudgel line (**Supplementary figure 1b,c**). Experiments were carried on using mosquitoes from G5 on.
426
427 **Transgene insertion mapping by inverse PCR**
428 Genomic Fudgel DNA was extracted from five homozygous male pupae using the Monarch DNA
429 purification kit (New England Biolabs ref T3010S/L) and quantified with Nanodrop. Extracted DNA (1µg)
430 was digested with AarI, AgeI, ApeI, SacII and XhoI restriction enzymes (FastDigest — Thermo
431 Scientific) for 1 hour at 37°C and enzymes were inactivated for 10 minutes at 80°C. The digested DNA
432 was diluted and treated with T4 DNA ligase (50 Units of enzyme for a 500µL reaction, Thermo Scientific
433 ref EL0011) overnight at room temperature. DNA was then purified using the Macherey-Nagel
434 NucleoSpin Gel and PCR Clean-up kit (ref 11992242) and amplified by nested-PCR using the
435 ThermoFisher Scientific DreamTaq DNA polymerase (ref EP0701). Primers for both PCR reations were

436 designed to amplify the 3' region of the transgene (**Supplementary table 8**). 15µL of the PCR were
437 Sanger sequenced (GATC Biotech, Eurofins) and the obtained sequence blasted on the AaegL5
438 LVP_AGWG reference genome on VectorBase. This alignment returned 1 hit on chromosome 3
439 (AaegL5_3:251028673:f). Deduced flanking genomic sequences were confirmed on both the 5' and 3'
440 sides of the *piggyBac* element by PCR amplification using the ThermoFisher Scientific Dreamtaq Green
441 MasterMix (ref K1081) (primers in **Supplementary table 8**) and sequenced (GATC Biotech, Eurofins).
442
443 **Salivation protocol optimization**
444 Fudgel female mosquitoes were starved 24h prior to experiment, then anesthetized with CO_2 and kept
445 on ice. Legs and wings were removed, and proboscis inserted in tips containing 10µL of FBS (Fetal
446 Bovine Serum). Mosquitoes were left to salivate either 30 minutes, 1 hour or 2 hours, then saliva
447 samples were collected. Each mosquito was considered a biological replicate.
448
449 **Marker detection and quantification by Western Blot**
450 Saliva samples were diluted 1:10 in 1x Laemmli Buffer and heated for 20 minutes at 95°C. Heating
451 process was repeated depending on experimental set up. Samples were then resolved on Mini-
452 PROTEAN TGX Stain-Free Precast Gel 4-15% (Bio Rad ref #4568086) and transferred to a
453 Nitrocellulose membrane (Trans-Blot Turbo Transfer Pack Bio Rad ref #1704158). Membranes were
454 blocked with 5% BSA (Albumine, from bovine serum SIGMA ref A3059) in PBS-Tween 0.1% solutions
455 and treated with either @HA-HRP (Roche ref 12013819001) or @V5-HRP (Invitrogen ref 46-0708)
456 antibodies 1:5000 in 1.5% BSA in PBS-Tween 0.1%. Membranes were incubated in the antibody
457 solution under agitation either 1 hour at room temperature or overnight at 4°C, rinsed in PBS-Tween
458 0.1%. Protein signal was revealed with ECL Select (Cytiva ref GERPN2235) using a ChemiDoc imaging
459 system (BioRad). Western Blot images were treated with the ImageJ software. Rectangular selection
460 of signal from all samples of the membrane constitutes a "lane": *Analyze/Gels/Select First Lane*. Bands
461 intensity was then plotted: *Analyze/Gels/Plot Lanes*, and relative band intensities recovered with the
462 *Wand* tool. Intensity values were then recorded, plotted on a log10 scale, and processed with the
463 RStudio software with the *ggplot2* and associated packages[50,51]. Saliva tag signal levels between
464 conditions were compared using a Kruskal-Wallis test.
465
466 **Fluorescent marker imaging**
467 Mosquitoes were anaesthetized with CO_2 and kept on ice. Whole body and proboscis images were
468 acquired on a Nikon SMZ18 fluorescent binocular microscope with sola light engine Lumencor® (**Figure**
469 **1d,f**). For salivary gland acquisitions (**Figure 1e**), dissections were performed in PBS under a
470 fluorescence microscope and the salivary glands were fixed in PFA 4% for 1h40 at room temperature
471 (RT). Samples were then permeabilized in PBS-T (0.2% Triton X-100, 1% BSA) for 45 minutes at RT
472 and incubated with DAPI (1:1000 in PBS-T) for 10 minutes at RT. Salivary glands were rinsed 3 x 10
473 minutes in PBS-T and mounted on slides using VECTASHIELD Antifade mounting medium (Vectorlabs,
474 ref H-1000). Acquisitions were performed on an epifluorescence microscope Axioskop 2 (Zeiss). For
475 confocal image acquisitions (**Supplementary figure 1d**) salivary glands and mosquito heads were

476 dissected in PBS under a fluorescent stereoscope. Fresh tissues were mounted in VECTASHIELD
477 mounting medium and confocal 10x Z stack acquisitions were performed using a spinning disk inverted
478 microscope (Zeiss, Axio Observer Z1). Stack images were merged using the "Extended Depth of Field"
479 plugin in ImageJ [52]: Direct Method, Expert Mode, EDF "Complex Wavelets". For proboscis, acquired
480 images were despeckled (*Process/Noise/Despeckle*) prior to merging to avoid signal loss.
481
482 **Salivation recording**
483 Mosquitoes were anaesthetized with CO_2 and kept on ice. Legs and wings were removed, and
484 proboscis inserted in FBS drops. Mosquitoes were left to salivate at room temperature for 1 hour.
485 Mosquitoes and droplets were then observed under a fluorescent microscope (Zeiss SteREO
486 Discovery.V8 microscope, X-Cite Xylis Excelitas Technologies laser) to witness salivation and for video
487 recording (**Supplementary video 1**).
488
489 **Physiological state and salivation**
490 5 to 8 days old Fudgel mosquitoes were blood-fed or not on mice anaesthetized with a solution of NaCl
491 0.9%, Rompun 2%, Zoletil 50. 3 days post-feeding fed females were given or not an egg dish to lay
492 their eggs. Egg dishes were removed after 3 days. Of note, blood-fed females without the egg dishes
493 had minor residual oviposition on the sugar pads. At day 7, day 10 and day 14 post-feeding, mosquitoes
494 were anaesthetized with CO_2, legs and wings removed, and females from the different feeding
495 conditions were put to salivate in 10µL FBS for 1 hour. 18 hours prior to salivation, mosquitoes were
496 starved by replacing sugar with water only. Non blood-fed Bangkok females of the same age were used
497 as negative control. Individual saliva samples were collected and diluted 1:10 in Laemmli 1x. The
498 samples were then analyzed by Western Blot with @V5-HRP antibody treatment.
499
500 **Salivary gland fluorescence intensity after natural blood feeding or forced salivation**
501 For blood feeding, mosquitoes were starved the prior day. Half of mosquitoes were allowed to fully
502 engorge on a mouse anaesthetized with a solution of NaCl 0.9%, Rompun 2%, Zoletil 50. For forced
503 salivation, mosquitoes were anaesthetized with CO_2 and kept on ice. Legs and wings were removed,
504 and half of them were put to salivate in 10µL FBS for 1 hour at RT. The salivary glands of control
505 mosquitoes, blood-fed mosquitoes, and mosquitoes that salivated were dissected under a fluorescent
506 binocular microscope (Nikon SMZ18 microscope, sola light engine Lumencor® laser). For each
507 condition of each replicate, between 6 and 8 salivary glands were dissected and analyzed. Pictures
508 were acquired with a fluorescent binocular microscope (Nikon SMZ18 microscope, sola light engine
509 Lumencor® laser). Fluorescence intensity quantification was done using ImageJ. For mTurquoise, YFP
510 and DsRed2, we calculated the Corrected Total Cell Fluorescence (CTCF):
511
512 $$CTCF_{marker} = fluorescence\ intensity - (Area\ x\ Background\ mean)$$
513
514 $$\rho CTCF = \frac{CTCF_{marker}}{CTCF_{DsRed2}}$$
515

516 Fluorescence intensity was normalized using ρCTCF, defined as the ratio between the CTCF value of
517 the salivation marker – either mTurq or YFP – and the CTCF of the DsRed2 transgenesis reporter.
518 ρCTCF for each marker of individual salivary glands are plotted using the *ggplot2* and associated
519 packages[50,51] on RStudio.
520
521 **Saliva detection in human skin explants**
522 Human skin explants were recovered from anonymized patients who underwent abdominal reduction
523 (St Anne Clinic, Strasbourg), with written informed consent and institutional review board approval, in
524 agreement with the Helsinki Declaration and French legislation. At reception, skin surfaces were wiped
525 successively with 70% ethanol, antiseptic solution (Dakin®) and phosphate buffer saline (Corning).
526 Superficial layers of the skins (200µm thickness) were harvested using a dermatome blade and
527 incubated in complete DMEM medium (10% fetal calf serum, 0.1mg/mL streptomycin, 100UI/mL
528 penicillin and 10µg/mL gentamycin) overnight at 37°C, 5% CO_2. The night prior to experiment, 5 female
529 mosquitoes were put in drosophila culture tubes and starved until the experiment. Human skins
530 explants were put in contact with starved mosquitoes and each batch of mosquitoes was allowed to
531 probe for 10 minutes. Different skin samples were then recovered, placed in 1x PBS and immediately
532 observed under a fluorescent binocular microscope (Nikon SMZ18 microscope, sola light engine
533 Lumencor® laser). Pictures were acquired using a Nikon DS-Ri2 camera.
534
535 **ZIKV and CHIKV infections**
536 One week old Bangkok and Fudgel female mosquitoes were transferred to a Biosafety Level 3
537 laboratory, anesthetized with CO_2 and kept on ice. Injections were performed using a Nanoject III micro-
538 injector (Dummond Scientific Company Cat. 3-000-207). Both ZIKV and CHIKV were tested in
539 independent experiments, in duplicates and triplicates respectively. Bangkok females were injected with
540 either 3000 PFU of ZIKV or 600 PFU of CHIKV in 100nL. Fudgel females were injected with either Mock
541 solution (virus growth medium: Gibco Leibovitz's L-15 Medium), or with 100nL of virus. They were left
542 to recover and incubate. Forced salivations were performed at either 14 days post-injection (dpi) or 9
543 dpi respectively for ZIKV and CHIKV.
544
545 **Forced salivation assays**
546 Mosquitoes were starved (deprived of sugar and water) the day before the experiment and anesthetized
547 with triethylamine (N,N-Diethylethanamine, SIGMA-Aldrich ref T0886). Legs and wings were removed,
548 and proboscis inserted in tips filled with 10µL FBS. Mosquitoes were left to salivate for 1 hour at RT.
549 Saliva samples and carcasses were then recovered for analysis. ZIKV and CHIKV RNA levels in
550 carcasses were measured by RT-qPCR (primers in **Supplementary table 8**). RNA was extracted using
551 the Mag-Bind Total RNA kit (Omega bio-tek ref M6731-01) at half-volumes and the KingFisher Apex
552 machinery (Thermo Scientific). Reverse transcription was performed using RevertAid H Minus enzyme
553 (Thermo Scientific ref EP0452) with random hexamers, and qPCR with PowerSYBR Green PCR Master
554 Mix (Applied Biosystems ref 4367659) and the reaction ran on Quant Studio 5 machinery (Applied
555 Biosystems). Results were processed using the apps.thermofisher.com platform and plotted with

556 *ggplot2* and associated packages[50,51] on RStudio. To quantify salivation levels, 2µL of each saliva
557 sample were mixed with 18µL of Laemmli 1x (1:10) and analyzed by Western Blot with @V5-HRP
558 antibody. Signal intensity was quantified using ImageJ and plotted with *ggplot2* and associated
559 packages[50,51] on RStudio.
560
561 Of the remaining saliva samples from CHIKV experiments, 5µL were used to perform an infection assay
562 on BHK cells. Cells were previously grown in DMEM medium (10% FBS, 1% Penicillin/Streptomycin
563 (P/S)) at 37°C, 5% CO2. 24h prior to infection, cells were diluted to 10^{-4} cells/100µL in DMEM medium
564 (5% FBS, 1% P/S) and sampled in 96 well plates. Saliva samples were diluted in series in DMEM
565 medium (0% FBS, 2% antibiotic-antimycotic, 1% P/S) and put on cells, from 10^{-2} to 10^{-7} dilution,
566 100µL/well, each dilution in quadruplicates. Viral stock dilutions from 10^{-4} to 10^{-9} in quadruplicates were
567 used as a positive control for cells infection. Non-infected saliva samples were used as negative
568 controls. Cells were left to incubate with the virus at 37°C, 5% CO_2. Cytopathic effect was measured
569 from 3dpi to 7dpi. For ZIKV saliva samples, 2µL of each individual saliva samples were used to infect
570 interferon-deficient A549 cells. Cells were grown and prepared as detailed for BHK cells. Saliva samples
571 were diluted in 100µL of DMEM medium (0% FBS, 2% antibiotic-antimycotic, 1% P/S) and put on cells
572 (50x dilution). Each saliva sample was used on one single cell well. Viral stock dilutions from 10^{-4} to 10^{-}
573 ^{9} in triplicates were used as a positive control for cells infection. Non-infected saliva samples were used
574 as negative controls. Cells were left to incubate with the virus at 37°C, 5% CO_2. Cytopathic effect was
575 measured from 3dpi to 7dpi.
576
577 ***In vivo* salivation assays**
578 Mosquitoes were starved (deprived of sugar and water) and B6.Cg-ifngr1tm1Agt ifnar1tm1.2Ees/J mice
579 were shaved on their abdomen and transferred to a Biosafety Level 3 laboratory the day before the
580 experiment. For the feeding experiment, mice were anaesthetized with a solution of NaCl 0.9%,
581 Rompun 2%, Zoletil 50. Mosquitoes – respectively 15 and 16 dpi for each experimental replicate – were
582 anesthetized with CO_2 and transferred into a 3D-printed individual females feeding system comprising
583 8 single-mosquito chambers (plans available on demand). Each feeder containing 8 individual female
584 mosquitoes was placed on the abdomen of a mouse and left feeding for ten minutes. After feeding,
585 mosquitoes were anesthetized with CO_2 and kept on ice. Engorgement status for each female was
586 noted, and carcasses were then recovered for analysis. ZIKV and CHIKV RNA levels in carcasses were
587 measured by RT-qPCR (primers in **Supplementary table 8**). RNA was extracted using the Mag-Bind
588 Total RNA kit (Omega bio-tek ref M6731-01) at half-volumes and the KingFisher Apex machinery
589 (Thermo Scientific). Reverse transcription was performed using RevertAid H Minus enzyme (Thermo
590 Scientific ref EP0452) with random hexamers, and qPCR with PowerSYBR Green PCR Master Mix
591 (Applied Biosystems ref 4367659) and the reaction ran on Quant Studio 5 machinery (Applied
592 Biosystems). Results were processed using the apps.thermofisher.com platform and plotted with
593 *ggplot2* and associated packages[50,51] on RStudio. Anesthetized mice were euthanized by cervical
594 dislocation and the bite sites on the abdomen skin regions were individually recovered with 8mm
595 disposable biopsy punches (Kai medical ref BP-80F) and put in TRIzol LS Reagent (Invitrogen ref

596 10296010). Proteins of individual skin samples were extracted using TRIzol Reagent Invitrogen protocol
597 (catalog numbers 15596026 and 15596018), resuspended in 200µL TrisHCl 50mM, SDS 1x, protease
598 inhibitor + EDTA and diluted in 200µL Laemmli buffer 2x (1:2). Individual skin protein samples were
599 analyzed by Western Blot with @V5-HRP antibody and @Actin Monoclonal Antibody (Invitrogen
600 mAbGEa ref MA1-744) 1:5000 in 1.5% BSA in PBS-Tween 0.1%.
601
602 **Microtome-slicing and immuno-fluorescence of ZIKV-infected mosquitoes**
603 Mosquitoes were anesthetized with CO_2 15 dpi and kept on ice. They were pre-fixed by injection of
604 100nl PFA 16% and fixed by immersion in PFA 4% for 2h at RT. They were then dehydrated by
605 successive baths in increasing concentration of sucrose solutions at RT: 12 hours in PBS 15% sucrose,
606 and 24h in PBS 30% sucrose. Dehydrated samples were pre-embedded for 48h at RT in liquid OCT
607 compound (Cellpath ref KMA-0100-00A). Embedding was done by immersing samples in liquid OCT
608 compound in plastic molds (Fisher Disposable Base Molds ref 22-363-353) and freezing in liquid
609 nitrogen. Samples were kept at -20°C. OCT blocks were microtome-sliced using a Cryostat system
610 (Leica CM3050 S) and 30µm slices were recovered on Clean SuperFrost slides (Epredia Superfrost
611 Plus Adhesion Microscope Slides ref J1800AMNZ). Slides were allowed to dry 2h at RT, immersed in
612 ice cold acetone for 30 minutes at RT and dried for 30 minutes. Each sample was circled with a
613 hydrophobic barrier pen (ThermoFisher ReadyProbes Hydrophobic Barrier Pap Pen ref R3777).
614 Samples were blocked with PBS-BSA 2% 2 times 10 minutes at RT and permeabilized in PBS-BSA 1%
615 + Triton 0.1% for 45 minutes at RT. Samples were incubated in primary antibody against ZIKV (mouse
616 4G2, laboratory synthetized stocks) at 1:50 in PBS-Triton 0.1% overnight at 4°C and washed 3 times
617 10 minutes in PBS-Triton 0.1%. Samples were blocked and permeabilized in PBS-BSA 1% + Triton
618 0.1% for 45 minutes at RT, and incubated in secondary antibody (Invitrogen Alexa Fluor 647 goat anti-
619 mouse IgG ref A21235) for 2h at RT. They were then washed 2 times 10 minutes in PBS-Triton 0.1%
620 and incubated with DAPI at 1:500 in PBS-Triton 0.1% for 15 minutes at RT. They were washed once in
621 PBS-Triton 0.1%, mounted in VECTASHIELD mounting medium and confocal 20x Z stack acquisitions
622 were performed using a confocal microscope (Zeiss, Beam Path LSM980). Images were processed in
623 ImageJ. 10x images were adjusted using the “Enhance Contrast” tool (saturation 405nm channel
624 0.05%, 639nm channel 0.1%). The saliva marker patterns were analyzed following a mitochondrial
625 quantification method optimized by Hemel et al.[53]. 40x images were deconvoluted using the “Iterative
626 Deconvolve 3D” plugin in ImageJ[40] (20 iterations) and saliva aggregates were highlighted using the “2D
627 Threshold” tool on the “Mitochondria Analyzer” plugin[41]. The mean area (µm2) of mTurq aggregates in
628 Mock and ZIKV-infected salivary glands was extracted from the “2D Threshold” analysis, plotted using
629 the ggplot2 package on RStudio and analyzed using a Wilcoxon test, threshold 0.05. 63x stack images
630 were deconvoluted using the “Iterative Deconvolve 3D” plugin in ImageJ[40] (20 iterations) and saliva
631 aggregates were highlighted using a Otsu’s Thresholding method. Correlation tests were performed on
632 whole stacks using the “JaCoP” plugin[54]. As for representation, stack images were merged using the
633 “3D Project” tool.
634

Acknowledgements

We thank members of the Mosquito Immune Response team for comments and discussions and staff at UPR9022 and U1257 for technical support, and especially Marcela Celis for maintenance of mosquito lines. This work was supported by grants from Conselho Nacional de Desenvolvimento Científico e Tecnológico (CNPq) to J.T.M.; Fundação de Amparo a Pesquisa do Estado de Minas Gerais (FAPEMIG), Instituto Nacional de Ciência e Tecnologia de Vacinas (INCTV) to J.T.M.; Fonds régional de coopération pour la recherche FRCT2020 Région Grand-Est – ViroMod to J.T.M. and C. M.; Institute for Advanced Studies of the University of Strasbourg (USIAS fellowship 2019) to J.T.M.; Human Frontiers Since Program (RGP018/2023) to J.T.M.; Agence Nationale de la Recherche ANR-21-CE12-0024 and ANR-24-CE15-4470 to J.T.M. and , ANR-19-CE35-0007 to E.M. and J. T. M.. This study was financed in part by the Coordenação de Aperfeiçoamento de Pessoal de Nível Superior — Brasil (CAPES) — Finance Code 001 to J.T.M. This work of the Interdisciplinary Thematic Institute IMCBio, as part of the ITI 2021-2028 program of the University of Strasbourg, CNRS and Inserm, was supported by IdEx Unistra (ANR-10-IDEX-0002), by SFRI-STRAT'US project (ANR 20-SFRI-0012), and EUR IMCBio (IMCBio ANR-17-EURE-0023) under the framework of the French Investments for the Future Program to J.T.M.. L.S. was supported by fellowships from IMCBio and FRM (Programme Fin de Thèse FDT2024040 18199). H.M. was supported by a FRM Postdoctoral Fellowship (SPF202110013925). The funders had no role in study design, data collection and analysis, decision to publish, or preparation of the manuscript.

Author contributions

L.S., M.B. and J.T.M. designed the project. L.S., M.B., B.V., T.H.J.F.L., E.M. and F.A. performed experiments. L.S. and J.T.M. analysed the data. L.S. and J.T.M. wrote the paper. All authors discussed the results and edited the manuscript.

Competing interests

The authors declare no competing interests.

663 **References**

664

665 1. Liu-Helmersson, J., Brännström, Å., Sewe, M. O., Semenza, J. C. & Rocklöv, J. Estimating Past,
666 Present, and Future Trends in the Global Distribution and Abundance of the Arbovirus Vector
667 Aedes aegypti Under Climate Change Scenarios. *Front. Public Health* **7**, 148 (2019).
668 2. Messina, J. P. *et al.* The current and future global distribution and population at risk of dengue. *Nat.*
669 *Microbiol. 2019 49* **4**, 1508–1515 (2019).
670 3. Crawford, J. E. *et al.* Population genomics reveals that an anthropophilic population of Aedes aegypti
671 mosquitoes in West Africa recently gave rise to American and Asian populations of this major
672 disease vector. *BMC Biol.* **15**, 16 (2017).
673 4. Rose, N. H. *et al.* Dating the origin and spread of specialization on human hosts in Aedes aegypti
674 mosquitoes. *eLife* **12**, e83524 (2023).
675 5. Atoni, E. *et al.* The discovery and global distribution of novel mosquito-associated viruses in the last
676 decade (2007-2017). *Rev. Med. Virol.* **29**, e2079 (2019).
677 6. Bhatt, S. *et al.* The global distribution and burden of dengue. *Nat. 2013 4967446* **496**, 504–507
678 (2013).
679 7. Grabenstein, J. D. & Tomar, A. S. Global geotemporal distribution of chikungunya disease, 2011–
680 2022. *Travel Med. Infect. Dis.* **54**, 102603 (2023).
681 8. Kraemer, M. U. *et al.* The global distribution of the arbovirus vectors Aedes aegypti and Ae.
682 albopictus. *eLife* **4**, e08347 (2015).
683 9. Wu, P., Yu, X., Wang, P. & Cheng, G. Arbovirus lifecycle in mosquito: acquisition, propagation and
684 transmission. *Expert Rev. Mol. Med.* **21**, e1 (2019).
685 10. Raquin, V. & Lambrechts, L. Dengue virus replicates and accumulates in *Aedes aegypti* salivary
686 glands. *Virology* **507**, 75–81 (2017).
687 11. Vega-Rúa, A., Schmitt, C., Bonne, I., Krijnse Locker, J. & Failloux, A.-B. Chikungunya Virus
688 Replication in Salivary Glands of the Mosquito Aedes albopictus. *Viruses* **7**, 5902–5907 (2015).
689 12. Visser, I., Koenraadt, C. J. M., Koopmans, M. P. G. & Rockx, B. The significance of mosquito saliva
690 in arbovirus transmission and pathogenesis in the vertebrate host. *One Health* **16**, 100506 (2023).
691 13. Arnoldi, I. *et al.* A salivary factor binds a cuticular protein and modulates biting by inducing
692 morphological changes in the mosquito labrum. *Curr. Biol. CB* **32**, 3493-3504.e11 (2022).

693 14. Sun, P. *et al.* A mosquito salivary protein promotes flavivirus transmission by activation of
694 autophagy. *Nat. Commun.* **11**, 1–15 (2020).
695 15. Lefteri, D. A. *et al.* Mosquito saliva enhances virus infection through sialokinin-dependent vascular
696 leakage. *Proc. Natl. Acad. Sci.* **119**, e2114309119 (2022).
697 16. Conway, M. J. *et al.* Aedes aegypti D7 Saliva Protein Inhibits Dengue Virus Infection. *PLoS Negl.*
698 *Trop. Dis.* **10**, e0004941 (2016).
699 17. McCracken, M. *et al.* Aedes aegypti salivary protein "aegyptin" co-inoculation modulates dengue
700 virus infection in the vertebrate host. *Virology* **0**, 133–139 (2014).
701 18. Cox, J., Mota, J., Sukupolvi-Petty, S., Diamond, M. S. & Rico-Hesse, R. Mosquito bite delivery of
702 dengue virus enhances immunogenicity and pathogenesis in humanized mice. *J. Virol.* **86**, 7637–
703 7649 (2012).
704 19. McCracken, M. K., Christofferson, R. C., Chisenhall, D. M. & Mores, C. N. Analysis of Early Dengue
705 Virus Infection in Mice as Modulated by Aedes aegypti Probing. *J. Virol.* **88**, 1881–1889 (2014).
706 20. Conway, M. J. *et al.* Mosquito Saliva Serine Protease Enhances Dissemination of Dengue Virus
707 into the Mammalian Host. *J. Virol.* **88**, 164–175 (2014).
708 21. Schmid, M. A. *et al.* Mosquito Saliva Increases Endothelial Permeability in the Skin, Immune Cell
709 Migration, and Dengue Pathogenesis during Antibody-Dependent Enhancement. *PLOS Pathog.*
710 **12**, e1005676 (2016).
711 22. Novak, M. G., Ribeiro, J. M. C. & Hildebrand, J. G. 5-Hydroxytryptamine in the Salivary glands Of
712 Adult Female Aedes Aegypti and its Role in Regulation of Salivation. *J. Exp. Biol.* **198**, 167–174
713 (1995).
714 23. Ribeiro, J. M. C. & Valenzuela, J. G. The salivary purine nucleosidase of the mosquito, *Aedes*
715 *aegypti*. *Insect Biochem. Mol. Biol.* **33**, 13–22 (2003).
716 24. Heitmann, A. *et al.* Forced Salivation As a Method to Analyze Vector Competence of Mosquitoes.
717 *J. Vis. Exp. JoVE* 57980 (2018) doi:10.3791/57980.
718 25. Sanchez-Vargas, I., Olson, K. E. & Black, W. C. The Genetic Basis for Salivary Gland Barriers to
719 Arboviral Transmission. *Insects* **12**, 73 (2021).
720 26. Miller, M. R. *et al.* Characterizing and Quantifying Arbovirus Transmission by Aedes aegypti Using
721 Forced Salivation and Analysis of Bloodmeals. *Insects* **12**, 304 (2021).

722 27. Gloria-Soria, A., Brackney, D. E. & Armstrong, P. M. Saliva collection via capillary method may
723 underestimate arboviral transmission by mosquitoes. *Parasit. Vectors* **15**, 103 (2022).
724 28. Juhn, J. *et al.* Spatial mapping of gene expression in the salivary glands of the dengue vector
725 mosquito, Aedes aegypti. *Parasit. Vectors* **4**, 1 (2011).
726 29. Ribeiro, J. M. *et al.* An annotated catalogue of salivary gland transcripts in the adult female
727 mosquito, Ædes ægypti*. *BMC Genomics* **8**, 6 (2007).
728 30. Goldman, O. V. *et al.* Mosquito Cell Atlas: A single-nucleus transcriptomic atlas of the adult Aedes
729 aegypti mosquito. 2025.02.25.639765 Preprint at https://doi.org/10.1101/2025.02.25.639765
730 (2025).
731 31. Boppana, V. D., Thangamani, S., Adler, A. J. & Wikel, S. K. SAAG-4 is a Novel Mosquito Salivary
732 Protein that Programs Host CD4+ T Cells to Express IL-41. *Parasite Immunol.* **31**, 287–295 (2009).
733 32. Calvo, E. *et al.* Aegyptin, a Novel Mosquito Salivary Gland Protein Specifically Binds to Collagen
734 and Prevents its Interaction with Glycoprotein VI, Integrin α2β1 and von Willebrand Factor. *J. Biol.*
735 *Chem.* **282**, 26928–26938 (2007).
736 33. Mathur, G. *et al.* Transgene-mediated suppression of dengue viruses in the salivary glands of the
737 yellow fever mosquito, Aedes aegypti. *Insect Mol. Biol.* **19**, 753–763 (2010).
738 34. Chagas, A. C. *et al.* Collagen-binding protein, Aegyptin, regulates probing time and blood feeding
739 success in the dengue vector mosquito, Aedes aegypti. *Proc. Natl. Acad. Sci. U. S. A.* **111**, 6946–
740 6951 (2014).
741 35. Olmo, R. P. *et al.* Control of dengue virus in the midgut of Aedes aegypti by ectopic expression of
742 the dsRNA-binding protein Loqs2. *Nat. Microbiol.* **3**, 1385–1393 (2018).
743 36. Tung, G. A. & Fonseca, D. M. Internal and external drivers interact to create highly dynamic
744 mosquito blood-feeding behaviour. *Proc. R. Soc. B Biol. Sci.* **291**, 20241105 (2024).
745 37. Hamel, R. *et al.* Biology of Zika Virus Infection in Human Skin Cells. *J. Virol.* **89**, 8880–8896 (2015).
746 38. Surasombatpattana, P. *et al.* Dengue virus replication in infected human keratinocytes leads to
747 activation of antiviral innate immune responses. *Infect. Genet. Evol.* **11**, 1664–1673 (2011).
748 39. Wichit, S. *et al.* Aedes Aegypti saliva enhances chikungunya virus replication in human skin
749 fibroblasts via inhibition of the type I interferon signaling pathway. *Infect. Genet. Evol. J. Mol.*
750 *Epidemiol. Evol. Genet. Infect. Dis.* **55**, 68–70 (2017).

751 40. Dougherty, R. Extensions of DAMAS and Benefits and Limitations of Deconvolution in
752 Beamforming. in *11th AIAA/CEAS Aeroacoustics Conference* (American Institute of Aeronautics
753 and Astronautics, 2012). doi:10.2514/6.2005-2961.
754 41. Chaudhry, A., Shi, R. & Luciani, D. S. A pipeline for multidimensional confocal analysis of
755 mitochondrial morphology, function, and dynamics in pancreatic β-cells. *Am. J. Physiol. -*
756 *Endocrinol. Metab.* **318**, E87–E101 (2020).
757 42. Tchankouo-Nguetcheu, S. *et al.* Infection by chikungunya virus modulates the expression of several
758 proteins in Aedes aegypti salivary glands. *Parasit. Vectors* **5**, 264 (2012).
759 43. Chisenhall, D. M. *et al.* Infection with dengue-2 virus alters proteins in naturally expectorated saliva
760 of Aedes aegypti mosquitoes. *Parasit. Vectors* **7**, 252 (2014).
761 44. Rossignol, P. A., Ribeiro, J. M. & Spielman, A. Increased intradermal probing time in sporozoite-
762 infected mosquitoes. *Am. J. Trop. Med. Hyg.* **33**, 17–20 (1984).
763 45. Yamamoto, D. S., Sumitani, M., Kasashima, K., Sezutsu, H. & Matsuoka, H. Inhibition of Malaria
764 Infection in Transgenic Anopheline Mosquitoes Lacking Salivary Gland Cells. *PLoS Pathog.* **12**,
765 e1005872 (2016).
766 46. Wei Xiang, B. W. *et al.* Dengue virus infection modifies mosquito blood-feeding behavior to increase
767 transmission to the host. *Proc. Natl. Acad. Sci. U. S. A.* **119**, e2117589119 (2022).
768 47. Alves e Silva, T. L. *et al.* High-Resolution Proteomics Unveils Salivary Gland Disruption and Saliva-
769 Hemolymph Protein Exchange in Plasmodium-Infected Mosquitoes. *bioRxiv* 2025.02.28.640873
770 (2025) doi:10.1101/2025.02.28.640873.
771 48. Bahr, L. *et al.* Antibody response to Aedes aegypti D7L1+2 salivary proteins as marker of aggregate
772 vector exposure and correlate of dengue virus susceptibility. *bioRxiv*
773 https://doi.org/10.1101/2025.05.01.651659 (2025) doi:https://doi.org/10.1101/2025.05.01.651659.
774 49. Marois, E. *et al.* High-throughput sorting of mosquito larvae for laboratory studies and for future
775 vector control interventions. *Malar. J.* **11**, 1–9 (2012).
776 50. Patil, I. Visualizations with statistical details: The 'ggstatsplot' approach. *J. Open Source Softw.* **6**,
777 3167 (2021).
778 51. Xu, S. *et al.* Use ggbreak to Effectively Utilize Plotting Space to Deal With Large Datasets and
779 Outliers. *Front. Genet.* **12**, (2021).

780 52. Forster, B., Van De Ville, D., Berent, J., Sage, D. & Unser, M. Extended depth-of-focus for multi-
781 channel microscopy images: A complex wavelet approach. in *2004 2nd IEEE International*
782 *Symposium on Biomedical Imaging: Macro to Nano (IEEE Cat No. 04EX821)* vol. 2 660–663 (IEEE,
783 Arlington, VA, USA, 2004).
784 53. Hemel, I. M. G. M., Engelen, B. P. H., Luber, N. & Gerards, M. A hitchhiker's guide to mitochondrial
785 quantification. *Mitochondrion* **59**, 216–224 (2021).
786 54. Bolte, S. & Cordelières, F. P. A guided tour into subcellular colocalization analysis in light
787 microscopy. *J. Microsc.* **224**, 213–232 (2006).
788

789 **Supplementary Materials**
790
791 **Supplementary Figures**
792
793 **Supplementary figure 1-** Establishment and phenotypic characterization of the Fudgel transgenic line.
794
795 **Supplementary figure 2-** Quantification of saliva reporter levels by Western Blot.
796
797 **Supplementary figure 3-** Quantification of the saliva reporter in samples collected from mosquitoes in
798 different physiological states.
799
800 **Supplementary figure 4-** Individual replicate plots for @V5-mTurq detection in saliva samples
801 collected from mosquitoes in different physiological states.
802
803 **Supplementary figure 5-** Fluorescent images of salivary glands from Fudgel mosquitoes after natural
804 blood-feeding or forced salivation.
805
806 **Supplementary figure 6-** Western Blot membranes of saliva samples collected from mosquitoes
807 infected with ZIKV or CHIKV.
808
809 **Supplementary figure 7-** Comparative analysis of salivation performance and saliva infectivity from
810 mosquitoes infected with ZIKV or CHIKV, in individual replicates.
811
812 **Supplementary figure 8-** Comparative analysis of salivation performance after mosquitoes feeding in
813 mice.
814
815 **Supplementary figure 9-** Imaging of ZIKV and saliva reporters in whole mosquito mounts using the
816 Fudgel transgenic line.
817
818 **Supplementary figure 10-** Analyzing the localization of ZIKV and saliva markers in salivary glands
819 from Fudgel mosquitoes.
820
821 **Supplementary Tables**
822
823 **Supplementary table 1-** Top 50 genes expressed in the distal lateral lobes (dll) of the salivary glands
824 and associated dll averaged UMAP score.
825
826 **Supplementary table 2-** Salivary glands lobes-specifically expressed genes and associated
827 abundance in saliva.
828

829 **Supplementary table 3-** Western Blot raw data for V5-mTurq signal detection by Western Blot.
830
831 **Supplementary table 4-** Western Blot raw data for V5-mTurq detection in saliva samples upon different
832 physiological states.
833
834 **Supplementary table 5-** Salivary glands fluorescence quantification raw values and CTCF calculations
835 for purging measurement after natural blood-feeding or forced salivation.
836
837 **Supplementary table 6-** Western Blot raw data for V5-mTurq detection in saliva samples upon ZIKV
838 and CHIKV infection.
839
840 **Supplementary table 7-** qPCR raw data for ZIKV, CHIKV and mTurq RNA detection in mosquitoes
841 carcasses.
842
843 **Supplementary table 8-** Primers used for Fudgel genetic construct cloning, transgene insertion
844 mapping and qPCR.
845
846 **Supplementary table 9-** Mean area (µm2) comparison between mTurq clusters in Mock and ZIKV-
847 infected individual salivary glands.
848
849 **Supplementary Video**
850
851 **Supplementary video 1-** Live V5-mTurq detection in a Fudgel female proboscis upon forced salivation
852 in PBS.